**Supplementary information**

# Irradiance and Temperature Considerations in the Design and Deployment of High Annual Energy Yield Perovskite/CIGS Tandems

Ramez Hosseinian Ahangharnejhad,[1] Adam B. Phillips,[1] Kiran Ghimire,[1] Prakash Koirala,[1] Zhaoning Song,[1] Hashem M. Barudi,[1] Aron Habte,[2] Manajit Sengupta,[2] Randy J. Ellingson,[1] Yanfa Yan,[1] Robert W. Collins,[1] Nikolas J. Podraza,[1] Michael J. Heben[1]

[1] University of Toledo, Wright Center for Photovoltaics Innovation and Commercialization, Department of Physics and Astronomy, 2801 W. Bancroft St., Toledo, OH, 43606 USA
[2] National Renewable Energy Laboratory, 15013 Denver West Parkway, Golden, CO 80401, USA

**Photoconversion Efficiency Results**

The photoconversion efficiency (PCE) results given in Figure 2 were further investigated by exploring the parameters that are relevant to the function of the tandem cells in two- and four-terminal configurations. Figure S1 shows the PCE, $V_{oc}$, $J_{sc}$, and ratio of the photogenerated current of the top cell to the bottom cell for a two-terminal tandem with 1.24 eV bandgap bottom cell within the 300 to 650 nm thickness range for the top cell perovskite layer. The results indicate that the current matching condition (white shaded areas in panel (d)), which corresponds to the maximum current in the two-terminal tandem, yields the highest PCE. On the other hand, little to none dependency on the tandem $V_{oc}$ is observed in the tandem PCE results. This is due to smaller variation in the $V_{oc}$ for the bandgap range studied.

For four-terminal tandems the PCE of the tandem is given along with the top and bottom subcell PCEs as a function of perovskite layer bandgap and thickness within the 300 to 650 nm top cell perovskite thickness in Figure S2. Results indicate that maximization in the PCE of the four-terminal tandem does not align with the optimal parameters for either subcell. However, a balance in the photocurrent and voltage of the top and bottom subcells lead to the maximization of PCE in 4-termainal tandems.

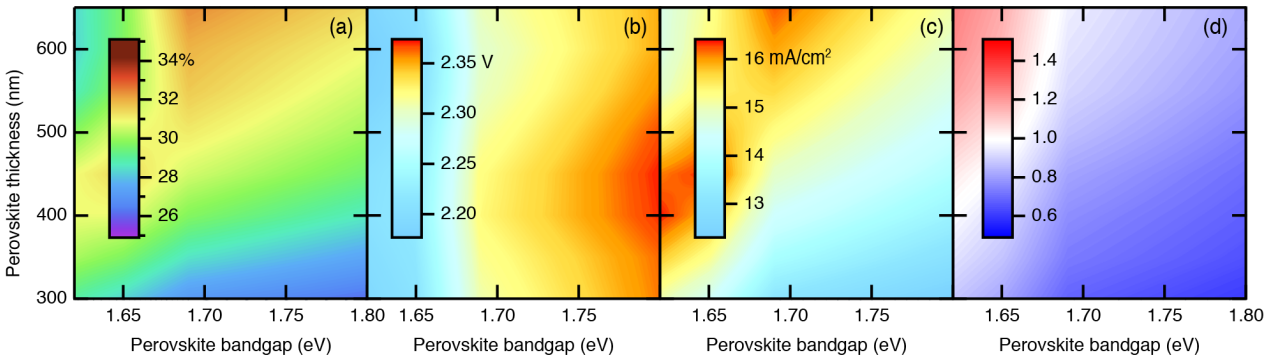


Figure S1. (a) PCE, (b) $V_{OC}$, (c) $J_{SC}$ of two-terminal tandems shown as function of top perovskite cell's bandgap and thickness. (d) Ratio of the photocurrent generated in the top to bottom subcells. Results shown in all panels correspond to the bottom CIGS cell with bandgap of 1.24 eV.

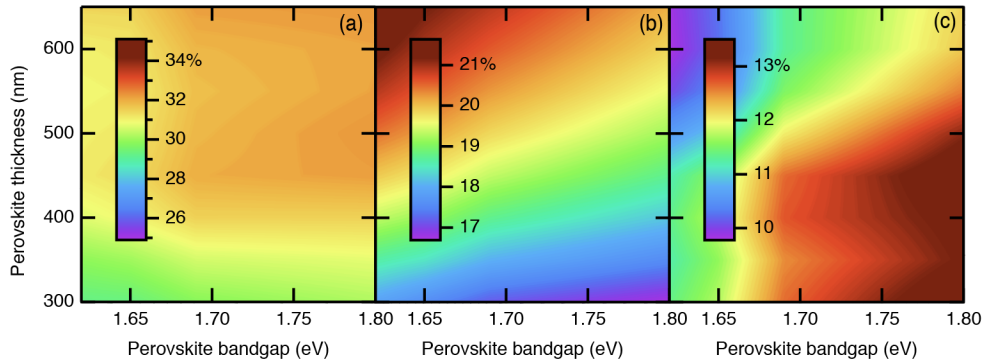


Figure S2. PCEs of the (a) four-terminal tandem, (b) top perovskite and (c) bottom CIGS subcells in the four-terminal tandem structure shown as function of top perovskite cell's bandgap and thickness. Results shown in all panels correspond to the bottom CIGS cell with bandgap of 1.24 eV.

**Methods of AEY calculation**

Figure S3 shows, computational flow chart for the AEY calculations where the irradiance, wind speed, and ambient temperature for every hour of the year is used to calculate the module temperature. Using the device structure and angle of incidence for either DNI or DHI light QE is determined. Module temperature and QE are used to calculate the reverse saturated current $J_0$, while the QE and irradiance (DNI or DHI) are used to calculate the photo generated current $J_{Ph}$. By implementing $J_0$, $J_{Ph}$ and series $R_s$ and shunt resistance $R_{sh}$ with ideality factor n (we assume ideality factor to be 1), into diode equation solution, current-voltage behavior is generated which is used to determine the maximum power point.

Temperature model

Figure S4 shows the effect of temperature model on the EY results. Panel (a) shows the percentage change in the generated power for a given two- and four-tandem cell with respect to the standard condition (25 °C). Results show a slight difference on the effect of temperature on operation of two-terminal tandem from the four-terminal one. Panel (b) shows the same for the module temperatures calculated at noon time of every day of a year for all the locations studied. While the module temperatures are calculated using the actual irradiance throughout a year, the efficiency calculations are performed using standard AM1.5 to isolate the effect of temperature on tandem cell

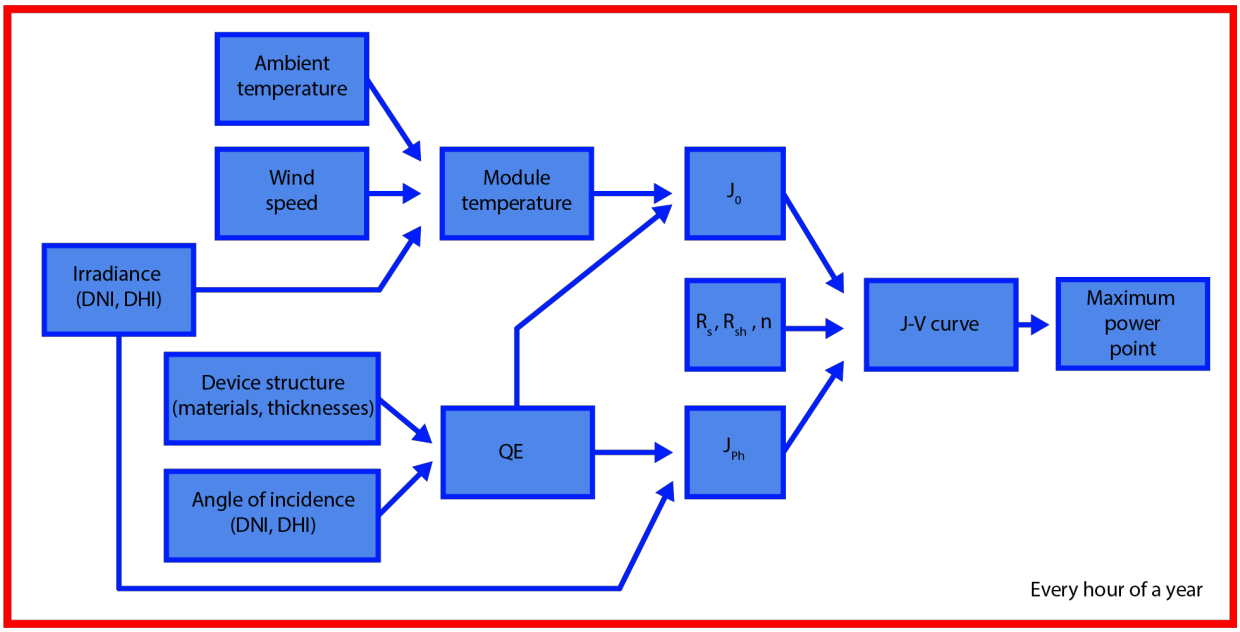


Figure S3. Computational flow chart used for the AEY calculation.

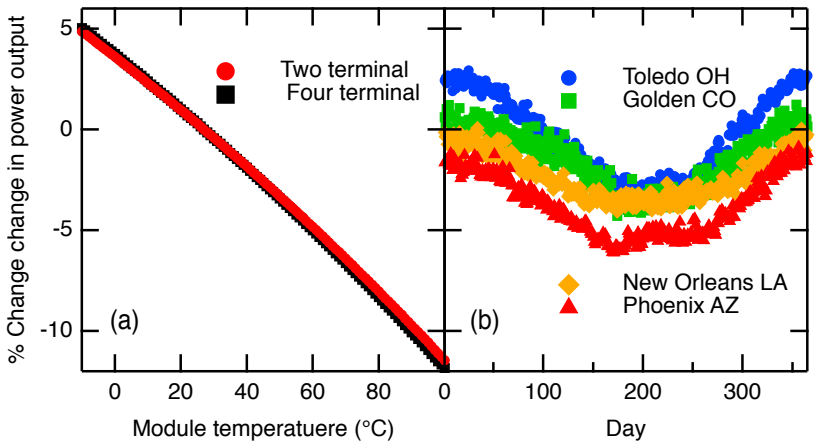


Figure S4. (a) Percentage change in the performance of modelled two- (red symbols) and four-terminal (black symbols) as a function of cell temperature relative to 25°C cell temperature. (b) Percentage change in the performance of modelled two-terminal cells at multiple locations with relative to 25°C at noon of everyday throughout a year.

operation. For colder climates such as Toledo OH, few percentage points improvements can be observed due to effect of temperature in winter months. However, for arid climate conditions such as Phoenix AZ, the effect of temperature is negative throughout the year and can yield reduced power output up to 6% with respect to the standard temperature conditions.

Irradiance data

Figure S5 shows the average irradiance data for Phoenix AZ and New Orleans LA. The data are presented with the AM 1.5 spectrum. To compare spectral composition with the standard AM1.5 spectrum, the average irradiances calculated for the two locations are normalized to overlap the given irradiance data for AM1.5. On the scale shown in the figure, the normalized average annual irradiances overlap the AM1.5 spectrum for these two locations. Using the average spectra shown here the monthly deviations are calculated which are given in figure 6 (c).

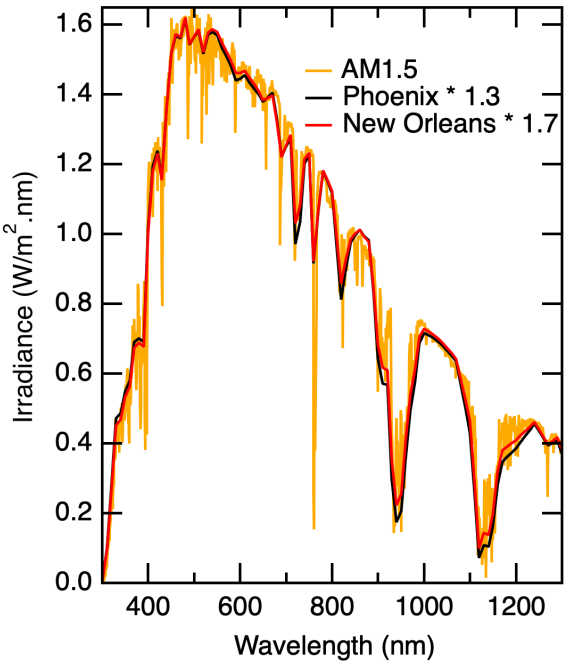


Figure S5. Average annual irradiance calculated for Phoenix AZ and New Orleans LA shown with AM1.5 irradiance. Average irradiances for two locations are normalized to match the AM1.5.

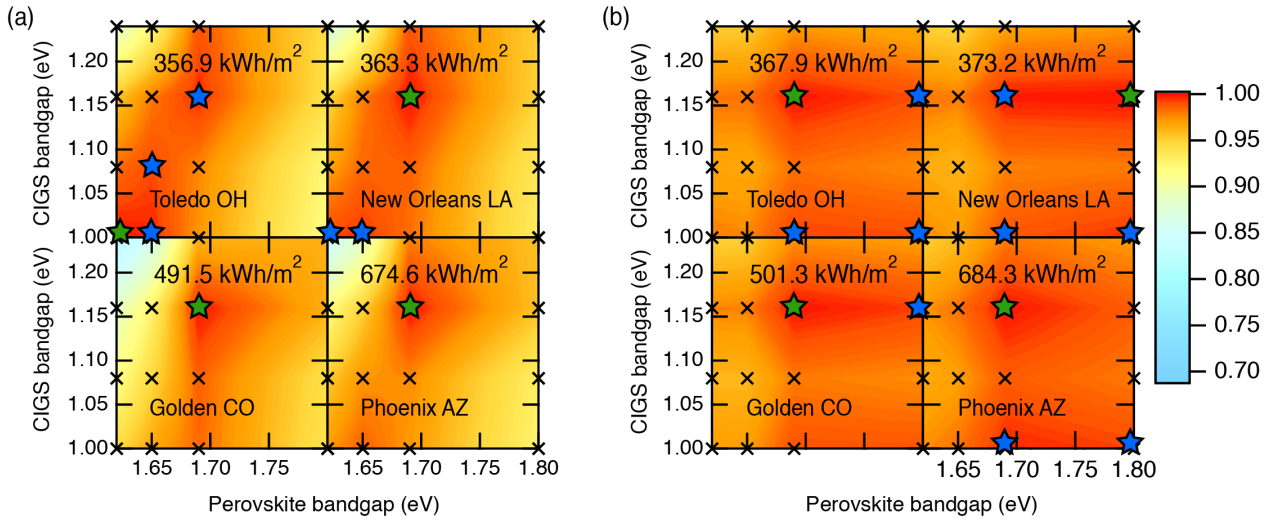


Figure S6. AEY results in four locations for (a) two- and (b) four-terminal tandems for 1-axis tracking with 650 nm and 500 nm thick perovskite layers respectively. Results in each panel are normalized to the maximum AEY (listed in each panel). The bandgap pairs with maximum AEY are identified with green stars while pairs with AEY within 1% of the maximum point are shown with blue stars.

**AEY results for tandem cells with thinner perovskite layer**

Figure S6, shows the results of annual energy yield (AEY) for two- and four-terminal tandem devices with 650 nm and 500 nm perovskite layers.

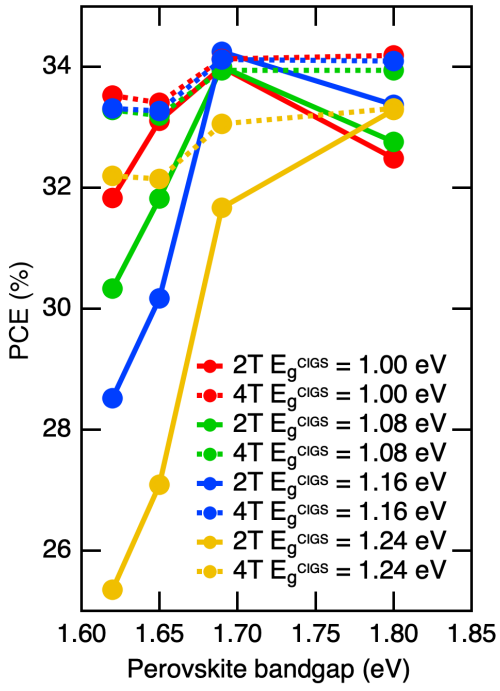


Figure S7. PCE of two- and four-terminal tandems with 1200 nm thick perovskite layers shown as a function of top cell bandgap for multiple bottom cell bandgaps with 1200 nm thick perovskite layer.

Supplementary information

| | Max 2T Annual Energy Yield (kW-hr-m$^{-2}$) | | | Max 4T Annual Energy Yield (kW-hr-m$^{-2}$) | | | 4T/2T Energy Production Ratio | | |
|---|---|---|---|---|---|---|---|---|---|
| | **OA** | **1A** | **2A** | **OA** | **1A** | **2A** | **OA** | **1A** | **2A** |
| **Toledo** | 284.6 | 373.1 | 405 | 292.9 | 381.2 | 414.1 | 102.92% | 102.17% | 102.25% |
| % of max | 70% | 92% | 100% | 71% | 92% | 100% | | | |
| **N.O.** | 302.4 | 379 | 426.7 | 308.4 | 388 | 436.1 | 101.98% | 102.37% | 102.20% |
| % of max | 71% | 89% | 100% | 71% | 89% | 100% | | | |
| **Golden** | 372.6 | 511.1 | 582.2 | 378.1 | 518.9 | 590 | 101.48% | 101.53% | 101.34% |
| % of max | 64% | 88% | 100% | 64% | 88% | 100% | | | |
| **Phoenix** | 558.4 | 698.3 | 781.8 | 574.4 | 706.6 | 793.6 | 102.87% | 101.19% | 101.51% |
| % of max | 71% | 89% | 100% | 72% | 89% | 100% | | | |

Table S1. Maximum AEY expected from two- and four-terminal tandem devices with no tracking, 1-axis and 2-axis tracking modes of operation. The ratio between two- to four-terminal maximum AEY for each mode of operation is given in addition to maximum AEY ratio between no tracking to 2-axis and 1-axis to 2-axis at each terminal configuration.

**Tandem devices with 1.2 $\mu$m perovskite**

Figure S7 shows the PCE of the two- and four-terminal tandem devices with 1200 nm thick perovskite layer. The PCE range is wider compared to the case of tandem devices with thinner perovskite layer shown in Figure 3. For these structures the maximum AEY results are given in Table S1. The results show that increased perovskite thickness leads to slightly higher AEY (between less than 1% to 5% increase).

Figure S8 shows the AEY results as functions of top and bottom subcell bandgap for the thicker perovskite layer. The devices over the narrow bandgap range of the top cell show significantly lower AEY than the maximum point. They also show a general shift in the optimal choice for bandgap pairs towards the wider range of bandgap pairs studied. The results also indicate that when the perovskite layer is thicker, the AEY is less tolerant to variations in absorber bandgap than when a thin perovskite layer is used.

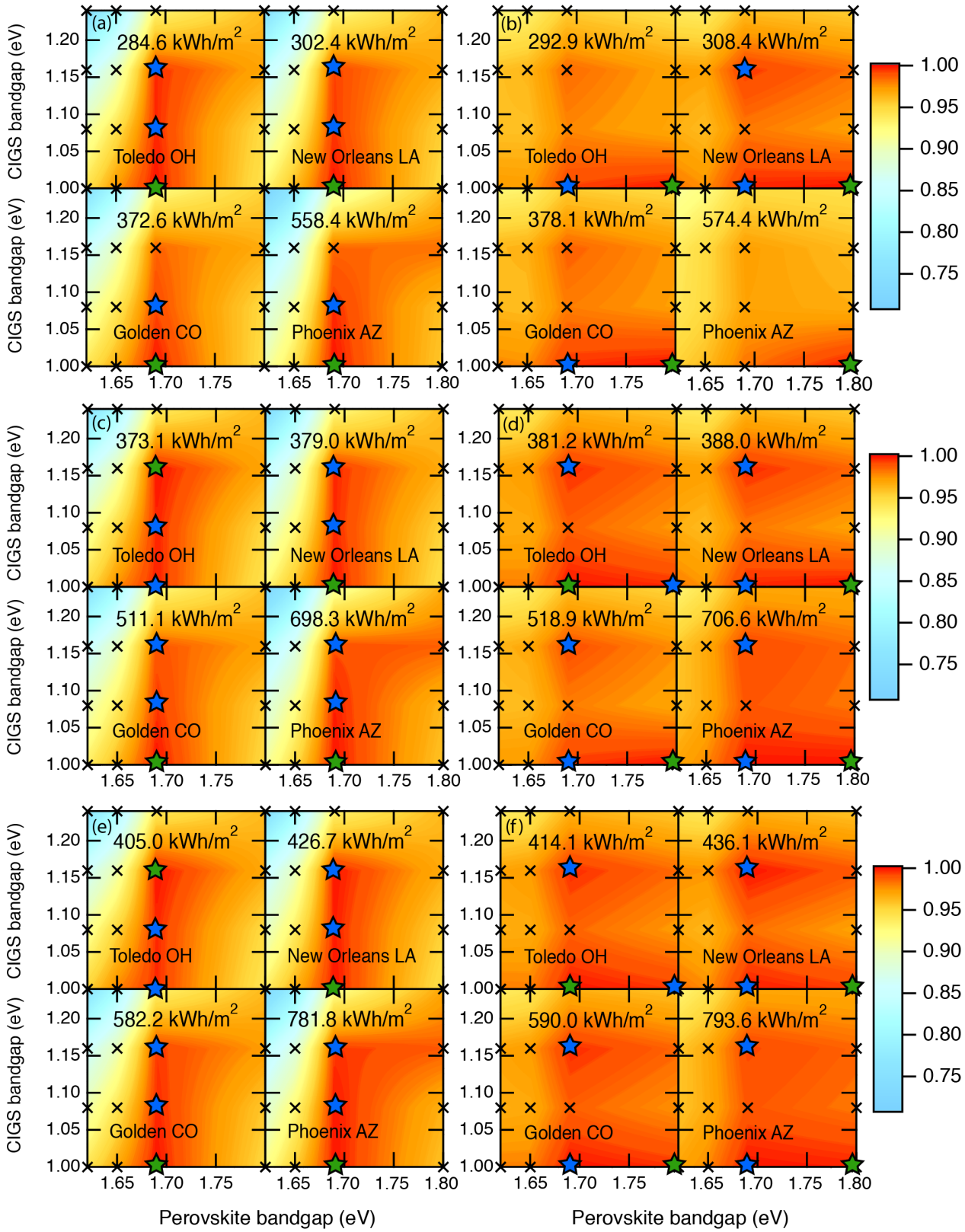


Figure S8. AEY shown for two- ((a), (c) and (e)) and four-terminal ((b), (d) and (f)) tandems with 1200 nm thick perovskite layer in 0- , 1- and 2- axis tracking modes respectively.